Lack of Metabolic Activation and Predominant Formation of an Excreted Metabolite of Nontoxic Platynecine−Type Pyrrolizidine Alkaloids

ARTICLE *in* CHEMICAL RESEARCH IN TOXICOLOGY · DECEMBER 2013

Impact Factor: 3.53 · DOI: 10.1021/tx4004159 · Source: PubMed

4 AUTHORS, INCLUDING:

Yang Ye
Chinese Academy of Sciences
139 PUBLICATIONS **2,023** CITATIONS
SEE PROFILE

Ge Lin
The Chinese University of Hong Kong
178 PUBLICATIONS **3,322** CITATIONS
SEE PROFILE

Chemical Research in Toxicology

Article

pubs.acs.org/crt

Lack of Metabolic Activation and Predominant Formation of an Excreted Metabolite of Nontoxic Platynecine-Type Pyrrolizidine Alkaloids

Jianqing Ruan,[†,‡] Cangsong Liao,[‡,§] Yang Ye,[‡,§] and Ge Lin*[,†,‡]

[†]School of Biomedical Sciences, Faculty of Medicine, The Chinese University of Hong Kong, Hong Kong SAR

[‡]Joint Research Laboratory for Promoting Globalization of Traditional Chinese Medicines between Shanghai Institute of Materia Medica, Chinese Academy of Sciences and The Chinese University of Hong Kong

[§]State Key Laboratory of Drug Research & Natural Products Chemistry Department, Shanghai Institute of Materia Medica, Chinese Academy of Sciences, People's Republic of China

Supporting Information

ABSTRACT: Pyrrolizidine alkaloid (PA) poisoning is well-known because of the intake of PA-containing plant-derived natural products and PA-contaminated foodstuffs. Based on different structures of the necine bases, PAs are classified into three types: retronecine, otonecine, and platynecine type. The former two type PAs possessing an unsaturated necine base with a 1,2-double bond are hepatotoxic due to the P450-mediated metabolic activation to generate reactive pyrrolic ester, which interacts with cellular macromolecules leading to toxicity. With a saturated necine base, platynecine-type PAs are reported to be nontoxic and their nontoxicity was hypothesized to be due to the absence of metabolic activation; however, the metabolic pathway responsible for their nontoxic nature is largely unknown. In the present study, to prove the absence of metabolic activation in nontoxic platynecine-type PAs, hepatic metabolism of platyphylline (PLA), a representative platynecine-type PA, was investigated and directly compared with the representatives of two toxic types of PAs in parallel. By determining the pyrrolic ester-derived glutathione conjugate, our results confirmed that the major metabolic pathway of PLA did not lead to formation of the reactive pyrrolic ester. More interestingly, having a metabolic rate similar to that of toxic PAs, PLA also underwent oxidative metabolisms mediated by P450s, especially P450 3A4, the same enzyme that catalyzes metabolic activation of two toxic types of PAs. However, the predominant oxidative dehydrogenation pathway of PLA formed a novel metabolite, dehydroplatyphylline carboxylic acid, which was water-soluble, readily excreted, and could not interact with cellular macromolecules. In conclusion, our study confirmed that the saturated necine bases determine the absence of metabolic activation and thus govern the metabolic pathway responsible for the nontoxic nature of platynecine-type PAs.

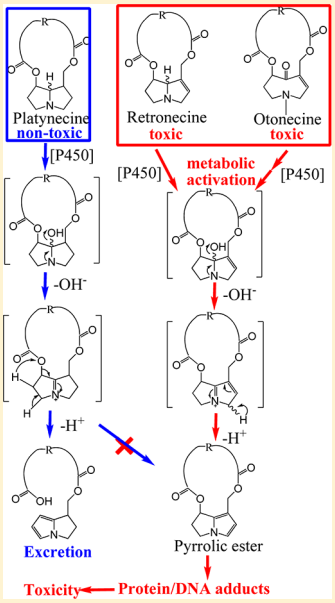

INTRODUCTION

Pyrrolizidine alkaloids (PAs) are common constituents of numerous plant species around the world. It has been reported that about 3% of the world's flowering plants contain toxic PAs.[1] More than 660 PAs have been identified in over 6000 plants distributed in many geographical regions worldwide, and most of them are hepatotoxic in humans and livestock.[2,3] Consequently, intake of PAs present in plants and/or contaminated in foodstuffs causes numerous cases of hepatotoxicity, especially hepatic sinusoidal obstruction syndrome worldwide, and PA poisoning cases are still reported yearly.[4,5] It has been reported that PAs are also tumorigenic, and the PA-induced tumor in experimental animals has been found through a genotoxic mechanism mediated by DNA adduct formation and levels of the DNA adducts correlated closely with the tumorigenic potencies in rats.[6−8]

PAs naturally occur as esters consisting of a necine base and a necic acid, as shown in Figure 1. Generally, based on different structures of the necine base, PAs are classified into three types: retronecine (including its 7-stereoisomer), otonecine, and platynecine type. Retronecine and otonecine types of PAs possessing a 1,2-double bond in the necine base are hepatotoxic and referred to as the unsaturated PAs, whereas the necine base in platynecine-type PAs does not have a double bond and has been reported to be nontoxic and regarded as saturated PAs.[2,3] The underlying mechanisms of the two toxic types of PAs have been well-established in that both of them were metabolically activated by hepatic cytochrome P450 enzymes to produce the dehydropyrrolizidine alkaloid intermediates, which are also called pyrrolic esters (Figure 1). Pyrrolic esters are highly

Received: May 6, 2013
Published: December 5, 2013

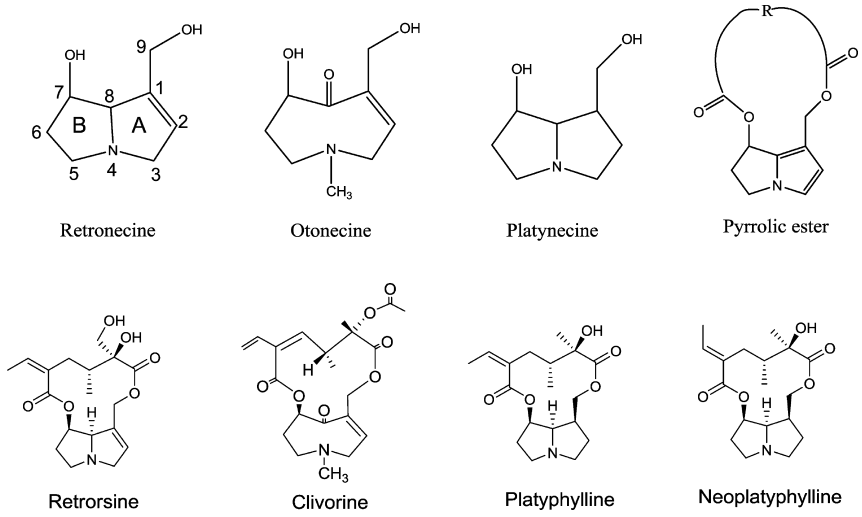

Figure 1. Structures of the common necine bases of different types of PAs, pyrrolic ester, and PAs investigated in the present study.

reactive alkylating agents. Once generated in the liver, pyrrolic esters rapidly bind to nucleophilic cellular macromolecules such as proteins or DNAs at C-7 and/or C-9 to form pyrrole−protein or pyrrole−DNA adducts, leading to hepatotoxicity or liver tumors, respectively.[2,3,9] On the other hand, depending upon the available amount of hepatic reduced form of glutathione (GSH), pyrrolic esters can also bind to GSH to form mono-GSH (7-glutathionyldehydroretronecine, GSM) and di-GSH conjugate (7,9-diglutathionyldehydroretronecine, GSD) until the GSH depletion.[10] Both GSH conjugates are nontoxic and readily excreted, and thus glutathione conjugation is regarded as the detoxification pathway. Due to the high reactivity, pyrrolic esters cannot be directly determined both in vivo and in vitro. Therefore, as well-established previously,[11,12] the formations of these GSH conjugates in vivo and in vitro (with excess amount of GSH added in the system) are proportional to the formation of pyrrolic esters, and thus the measured quantities of these conjugates can represent the toxic potency of PAs.

Nontoxic platynecine-type PAs are frequently present together with toxic retronecine-type PAs in plants.[13] A few animal studies in early years (1939−1968) reported that platynecine-type PAs, such as rosmarinine and platyphylline, were not hepatotoxic,[14,15] and even at acute sublethal dose, platyphylline did not cause significant hepatic or renal damages in the treated mice, rats, or guinea.[16] Based on these findings, the saturated platynecine-type PAs have been recognized as nontoxic PAs for a long time and the saturated necine base was suspected not to undergo the metabolic activation in this type of nontoxic PA.[14] However, compared to the well-investigated toxic types of PAs, studies on the nontoxic PAs are limited. To date, for platynecine-type PAs, whether the metabolic activation is absolutely absent and, if it is absent, whether other metabolic pathways occur and to what extent are largely unknown, although such a metabolic pathway would be responsible for the nontoxic nature of platynecine-type PAs. In the present study, the hepatic metabolism of platyphylline, a representative platynecine type of PA, was investigated and also compared with the representative PAs in each of the two toxic types of PAs to determine their differences in hepatic metabolism. In particular, the metabolic activation was quantitatively determined and directly compared between toxic and nontoxic PAs in the parallel study, and the metabolic pathway responsible for the nontoxicity of platynecine-type PAs was thoroughly investigated to reveal distinctive features of hepatic metabolism of nontoxic platynecine-type PAs.

MATERIALS AND METHODS

Materials. Retrorsine (RET, the representative of retronecie type PA, Figure 1), GSH, and all other chemicals were purchased from Sigma Chemical Co. (St. Louis, MO). Clivorine (CLI, the representative of otonecine type PA, Figure 1) was isolated from *Ligularia hodgsonii* Hook in our laboratory.[17] Platyphylline (with 30% of its isomer neoplatyphylline (NPLA), Figure 1) was a gift from Prof. H.S. Chen at the Department of Phytochemistry, The Secondary Military Medical University, China.[12] GSM and GSD standards were isolated from the scaled-up rat hepatic microsomal incubation as reported previously.[12] The rat hepatic subcellular fractions including S9, cytosol, and microsome fraction were prepared using standard methods described previously.[12] Human liver microsomes and recombinant human supersomes were purchased from BD Gentest (Woburn, MA). The content of cytochrome P450 in both rat and human liver microsomes was determined to be 1 nmol/mg protein using the Omura methods.[18] HPLC-grade acetonitrile and methanol purchased from Merck (Darmstadt, Germany) were used for HPLC analyses.

Metabolic Incubation and Sample Preparation. Individual PAs at 200 μM were incubated with rat hepatic S9, microsomes, or human liver microsomes (2 mg protein/mL) in a reaction mixture (0.2 mL) containing 100 mM potassium phosphate buffer (pH 7.4), a NADPH-regenerating system (5 mM $MgCl_2$, 1 mM $NADP^+$, 1 mM G-6-P, and 1 U/mL G-6-PD), and 2 mM of GSH, which is added with excess amount as a trapping agent to bind the reactive pyrrolic esters to form GSH conjugates. Incubations without the NADPH-regenerating system or PAs served as controls. After incubation for 2 h, the reactions were stopped at 4 °C and the samples were then immediately centrifuged at 15 000*g* for 20 min at 4 °C. The filtered supernatant was filtered through a 0.45 μm membrane filter before being subjected to HPLC analysis.

Isolation and Identification of the Predominant Metabolite of PLA. The predominant metabolite (M3) was prepared by a scaled-up reaction with pooled rat liver S9 fraction. In brief, 20 mg of PLA was incubated with rat liver S9 (1 mg protein/mL) in a reaction mixture of 100 mL of potassium phosphate buffer (pH 7.4) at 37 °C for 4 h. After addition of 100 mL of ice-cold acetonitrile, the samples were centrifuged at 5000*g* and 4 °C for 30 min. The resultant supernatant was concentrated under reduced pressure and loaded on a semipreparative column (Jones chromatography Apex octadecyl, 250 mm × 10 mm) for the purification. The fractions containing M3 were collected, concentrated, and lyophilized. A yellow powder was

dx.doi.org/10.1021/tx4004159 | *Chem. Res. Toxicol.* 2014, 27, 7−16

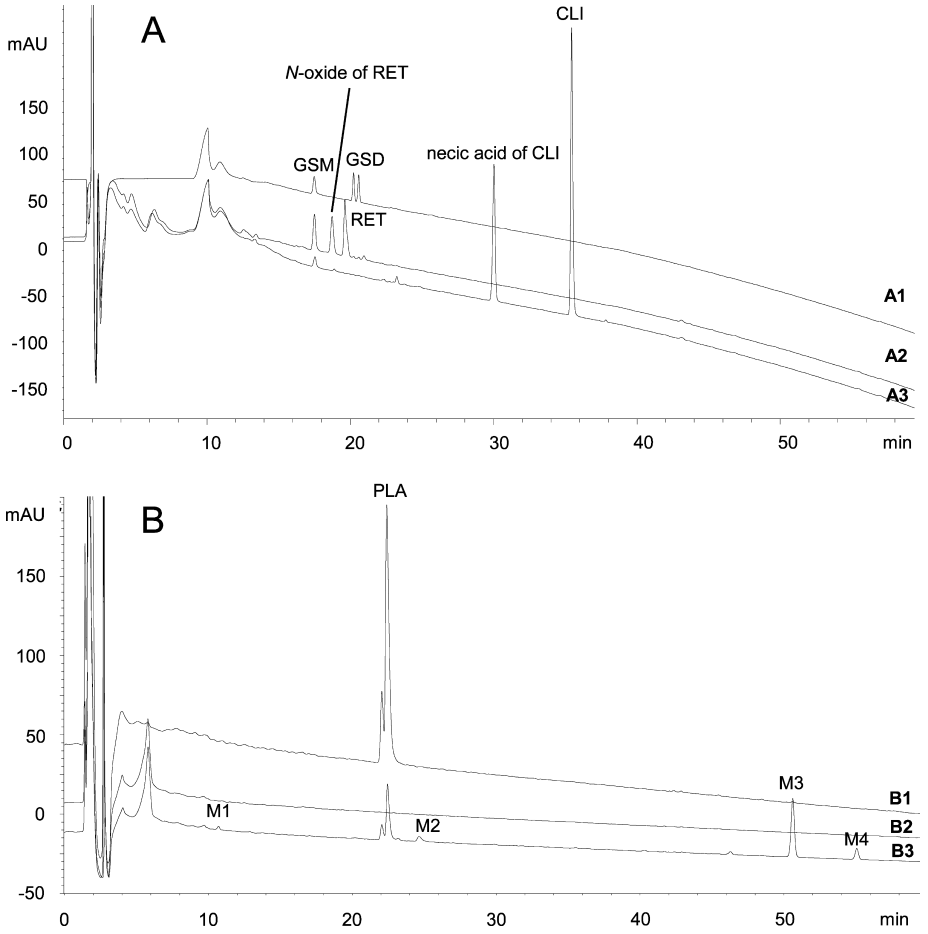

Figure 2. Representative chromatograms of HPLC-UV analysis of GSM and GSD standards (A1), rat liver S9 incubation of RET (A2) and CLI (A3) in the presence of GSH, control rat liver S9 incubation spiked with PLA standard (B1), control rat liver S9 incubation (B2), and rat liver S9 incubation of PLA in the presence of GSH (B3).

obtained with 25% yield. The fractions were monitored using HPLC-UV during preparation, and the purity of the obtained metabolite was >90% as determined by HPLC-UV analysis.

The structure of the purified metabolite M3 dissolved in $CDCl_3$ (Cambridge Isotope Laboratories, Inc.) was determined by NMR analyses, including ^1H, ^{13}C, HSQC, HMBC, and ROESY. ROESY experiment was recorded on a Varian MR-400, and other experiments were recorded on a Bruker AVANCE III-500. Chemical shifts were given on δ scale and referenced to $CDCl_3$ at 7.26 ppm for ^1H NMR (500 MHz) and 77.16 ppm for ^{13}C NMR (125 MHz).

Identification of Rat Hepatic Enzymes Mediating Metabolism of PLA. Specific inhibitory study was conducted to identify the rat hepatic enzymes mediating metabolism of PLA according to our previously developed method with minor modification.[19] Different inhibitors were used including SKF 525A (a nonselective inhibitor of P450, 100 μM), methimazole (a nonselective inhibitor of flavin-containing mono-oxygenases (FMOs), 100 μM), 8-methoxypsoralen (an inhibitor of P450 2A2, 100 μM), metyrapone (an inhibitor of P450 2B, 50 μM), cimetidine (an inhibitor of P450 2C6/11, 100 μM), α-naphthoflavone (an inhibitor of P450 1A1/2, 50 μM), quinine (an inhibitor of P450 2D, 100 μM), diethyldithiocarbamate (an inhibitor of P450 2E1, 200 μM), and ketoconazole (an inhibitor of P450 3A, 10 μM). The incubation conditions were the same as described above except for the preincubation with individual inhibitors for 15 min and using rat liver microsomes.

Identification of Human P450s Mediating Metabolism of PLA. PLA was further incubated with human liver microsomes and individual recombinant P450 1A1, 1A2, 2B6, 2C9, 2C19, 2D6, and 3A4, in order to identify the roles of human P450 enzymes. All experiments were conducted at 37 °C for 2 h at a final protein concentration of 150 pmol/mL (supersomes) and 2 mg/mL (human liver microsomes), respectively.

HPLC-UV and HPLC-MS/MS Analyses. Quantitative analysis of the intact PLA and its metabolites was conducted on an Agilent series 1100 HPLC system (Agilent Technologies, Santa Clara, CA, USA) equipped with a vacuum degasser, a binary pump, an autosampler, and a diode array detector. Sample analysis was performed on a Waters Symmetry C_{18} column (150 mm × 4.6 mm, 5 μm). The column temperature was maintained at 25 °C, and the flow rate was set at 1.0 mL/min. Injection volume was 50 μL. PLA and its metabolites were monitored at 230 nm, and their UV absorption spectra were recorded over 200−400 nm. The mobile phases consisted of 10 mM ammonium acetate water (A, adjusted the pH to 5 by acetic acid) and acetonitrile (B), and the gradient elution was 2−40% B from 0 to 60 min.

The MS analysis was performed on an API 2000 Q-Trap mass spectrometer (AB Sciex, USA) for the structural elucidation of metabolites of PLA. The mass spectrometer was operated in positive ion mode using an electrospray ionization interface with the following working parameters: ion spray voltage, 5500 V; curtain gas, 20 psi; gas 1, 30 psi; gas 2, 70 psi; and source temperature, 400 °C. All gases used were nitrogen. Declustering potential was set at 70 V, and entrance potential was set at 10 V. MS/MS conditions were as follows: collision energy, 30 V; and collision cell exit potential, 2 V.

The intact PAs and metabolites (M2 and M3) of PLA in the incubated samples (n = 3) were quantitatively measured by HPLC-UV analysis via constructing calibration curves using the corresponding standards. The metabolic rate of individual PAs was calculated as follows: percentage of metabolism = $(C_0 - C_{2h}/C_0) \times 100\%$, where C_0 is the concentration of the intact PA in the incubation mixture prior to

dx.doi.org/10.1021/tx4004159 | Chem. Res. Toxicol. 2014, 27, 7−16

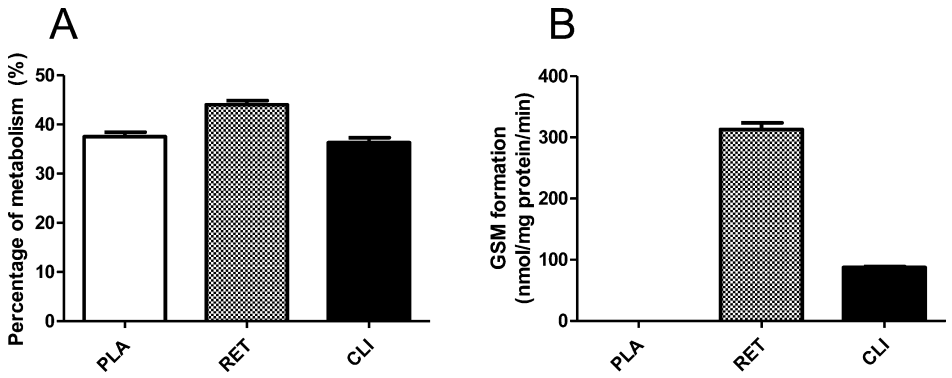

Figure 3. Percentage of metabolism (A) and GSM formation rate (B) of different PAs incubation with rat liver S9 in the presence of GSH.

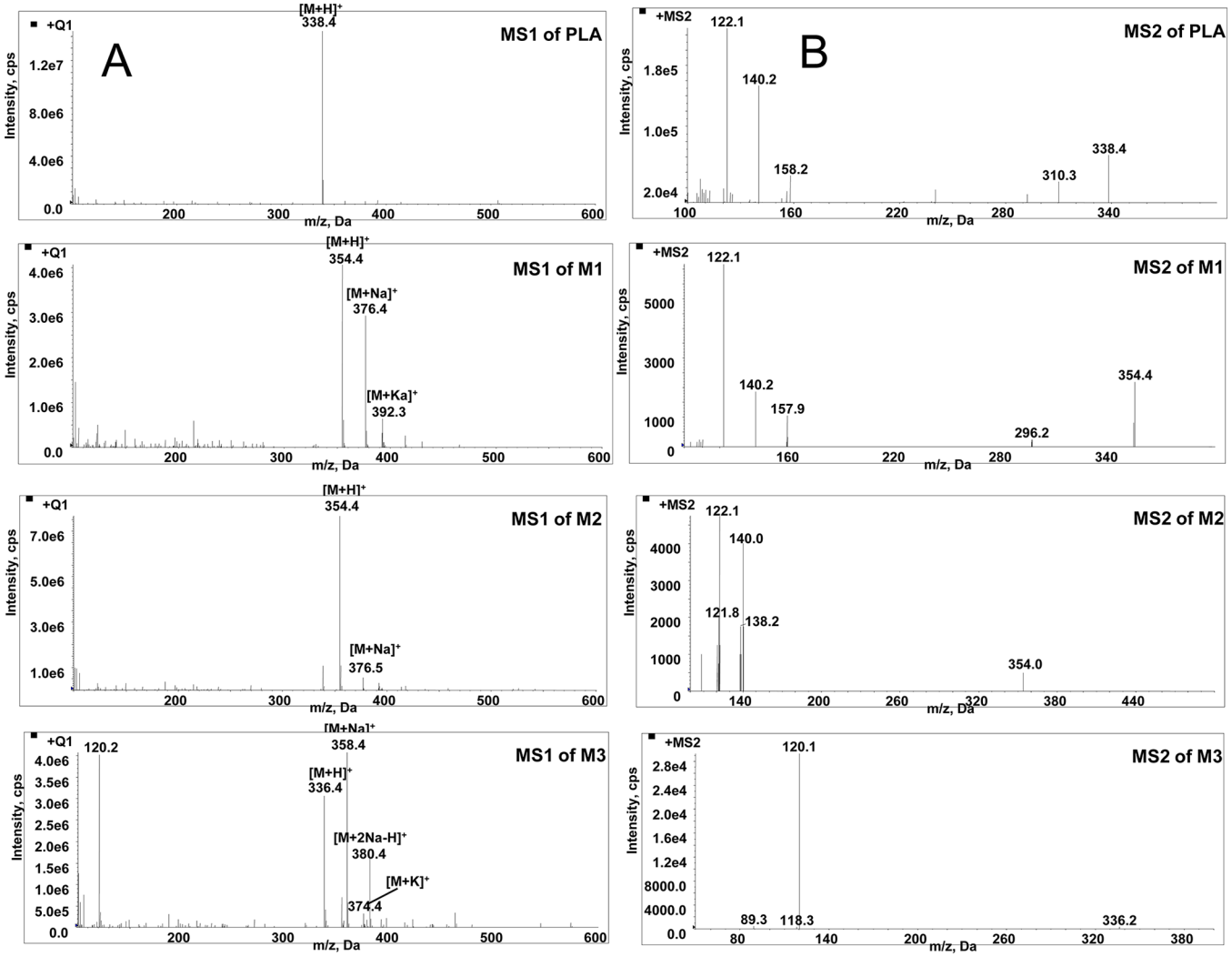

Figure 4. MS1 spectra of PLA and different metabolites (A) and MS2 spectra of PLA and different metabolites (B).

incubation and C_{2h} is the concentration of the intact PA in the incubation mixture after incubation for 2 h.

RESULTS

Rat Hepatic Metabolism of PLA with a Comparison of the Representatives of Two Toxic Types of PAs. As shown in Figure 2, GSM was determined after incubation of RET and CLI (Figure 2A) but not PLA (Figure 2B) with rat hepatic S9, indicating that the metabolic activation to form the reactive pyrrolic esters only occurred in both types of toxic PAs but not in the nontoxic PA. In addition, the corresponding *N*-oxide and the necic acid (clivoric acid), which were reported previously as the main metabolite of RET and CLI, respectively, were also found in the present study.[11,20] More interestingly, the metabolic rates of all three different types of PAs tested were similar (37% PLA, 44% RET, 36% CLI, Figure 3A), while the formation rate of GSM, which corresponded to the formation rate of reactive metabolic intermediates, varied

dx.doi.org/10.1021/tx4004159 | Chem. Res. Toxicol. 2014, 27, 7−16

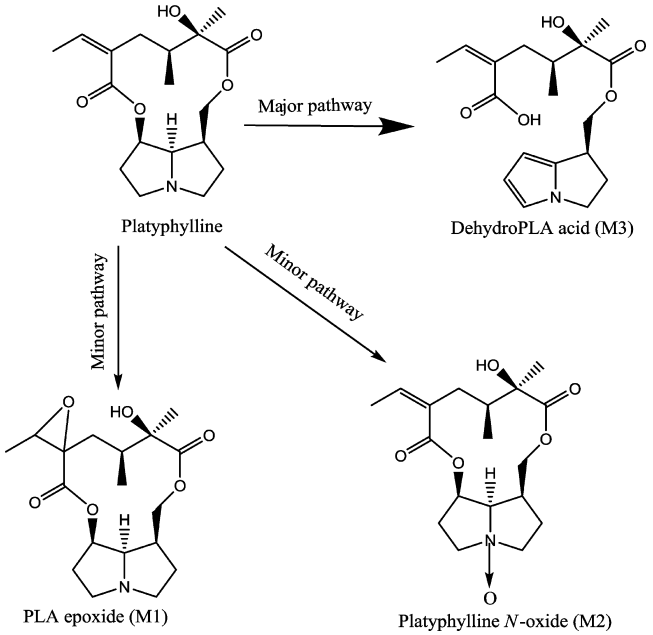

Figure 5. Proposed in vitro hepatic metabolic pathways of PLA.

significantly with the highest production by RET but no formation in PLA (Figure 3B). Furthermore, several metabolites of PLA were formed in the presence of NADPH-regenerating system but not in different controls, demonstrating that all metabolites formed were microsomal enzyme-dependent.

As observed in the HPLC-UV chromatograms (Figure 2B), apparently four putative metabolites with M3 as the predominant one were formed after PLA incubation. These metabolites were further analyzed by HPLC-MS/MS. As shown in the MS1 spectra (Figure 4A), both M1 and M2 showed quasi-molecular ions $[M + H]^+$ at m/z 354, 16 Da higher than that of PLA, indicating that they were the oxidized metabolites of PLA. The further MS/MS analysis of M1 (Figure 4B) exhibited ion pairs at m/z 122 and 140, which were the characteristic ion pairs of the necine base of the saturated PAs,[21] confirming the intact necine base. Therefore, oxidation was most likely at the necic acid, and M1 was identified as PLA epoxide (Figure 5). In the case of M2, its MS2 spectrum showed the characteristic PA *N*-oxide ion clusters at m/z 120−122 and 138−140,[22] confirming that M2 was PLA *N*-oxide (Figure 5). For the predominant metabolite M3, its MS1 and MS2 spectra showed a similar pattern to those of M4 with identical pseudomolecular ions and fragmentation ions. Considering the PLA sample examined containing 30% of its isomer NPLA and their apparently compatible peak area ratio in the HPLC-UV chromatogram (Figure 2B), M3 and M4 were suspected and subsequently proven by HPLC-MS/MS analysis (MS1 and MS2 mass spectra of M4 are provided in Supporting Information Figure 1) as the same metabolite generated from PLA and NPLA, respectively.

The MS1 spectrum of M3 (Figure 4) exhibited protonated ions $[M + H]^+$ at m/z 336, $[M + Na]^+$ at m/z 358, and [M +

Table 1. ^{1}H Proton and ^{13}C NMR Chemical Shift Assignments of M3[a]

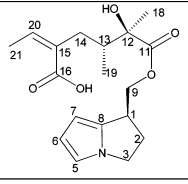	^{1}H	^{13}C
Carbon No.		
1	3.49, m	36.8
2	2.29, m 2.72, m	32.1
3	3.95, m 4.02, m	45.5
5	6.61, dd (1.2, 3.6)	114.3
6	6.22, dd (3.0, 3.6)	112.5
7	5.87, dd (1.2, 3.0)	100.1
8		136.5
9	4.16, dd (6.2, 10.5) 4.34, dd (7.5, 10.5)	67.5
11		177.7
12		76.6
13	2.04, m	39.5
14	2.01, m 2.37, m	37.3
15		130.0
16		170.1
18	1.33, s	24.1
19	0.91, d (6.6)	12.8
20	6.10, q (7.2)	141.9
21	2.01, d (7.2)	16.2

[a]Measured in $CDCl_3$: δ in ppm (multi, J in Hz).

dx.doi.org/10.1021/tx4004159 | *Chem. Res. Toxicol.* 2014, 27, 7−16

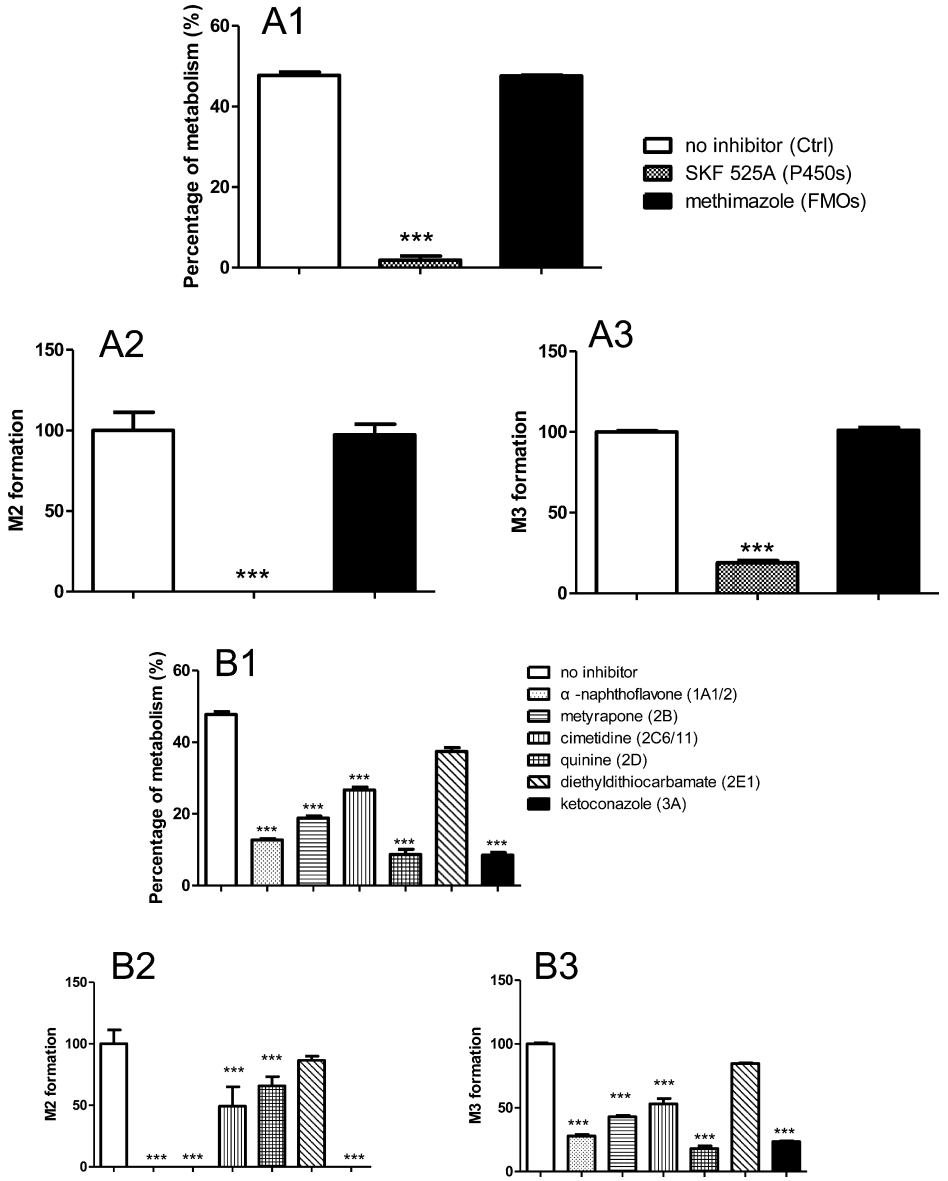

Figure 6. Percentage of metabolism (A1), M2 (A2), and M3 (A3) formation rates of PLA in rat liver microsomes in the presence of P450 and FMO inhibitors. Percentage of metabolism (B1), M2 (B2), and M3 (B3) formation rates of PLA in rat liver microsomes in the presence of different P450 inhibitors. M2 and M3 formation rates in the absence of inhibitors were normalized to be 100, while the percentage of M2 and M3 formation rates in the presence of different inhibitors was calculated by comparing with that in the absence of inhibitors; ***$p < 0.001$ compared with the control group without inhibitors ($n = 3$).

K]$^+$ at m/z 374, indicating its molecular weight of 335 with a loss of two hydrogen elements from PLA. Its MS2 spectrum showed a base peak at m/z 120, rather than the characteristic pairs of the saturated necine base ions at m/z 122 and 140, suggesting the altered saturated necine base. M3 was further elucidated by various NMR spectra (Supporting Information Figures 2−7). The ^{1}H and ^{13}C NMR data of M3 were very similar to those of PLA,[23,24] except for the low-fielded carbon signal at δ_C 170.1 in the ^{13}C NMR spectrum, suggesting the presence of a carboxylic acid instead of an ester group. HMBC correlations from H-9 [δ_H 4.16, dd (6.2, 10.5 Hz); δ_H 4.34, dd (7.5, 10.5 Hz)] to C-11 (δ_C 177.7) indicated that the ester group at C-11 remained, and the carboxylic acid was therefore located at C-16. The ^{13}C NMR spectrum also displayed characteristic resonances at δ_C 114.3 (C-5), 112.5 (C-6), 100.1 (C-7), and 136.8 (C-8), indicating the presence of both 5,6-double bond and 7,8-double bond. HMBC correlations from H-9 to C-1 (δ_C 36.8) and C-2 (δ_C 32.1) further suggested that these two double bonds are located at ring B of the necine base. Furthermore, the configuration of a 15,20-double bond remained the same as that of PLA and was deduced to be *Z* based on the correlation between H-14 and H-20 in the ROESY spectrum (Supporting Information Figure 7). Accordingly, M3 was unequivocally identified as hexanedioic acid, 5-ethylidene-2-hydroxy-2,3-dimethyl-1-[(2,3-dihydro- 1*H*-pyrrolizin-1-yl)methyl] ester, which is a novel metabolite and named dehydroplatyphylline carboxylic acid (dehydroPLA carboxylic acid, Figure 5). The detailed assignments of ^{1}H and ^{13}C NMR signals are summarized in Table 1. Similarly, M4 was identified as dehydroneoplatyphylline carboxylic acid (dehydroNPLA carboxylic acid), the predominant metabolite of NPLA.

dx.doi.org/10.1021/tx4004159 | *Chem. Res. Toxicol.* 2014, 27, 7−16

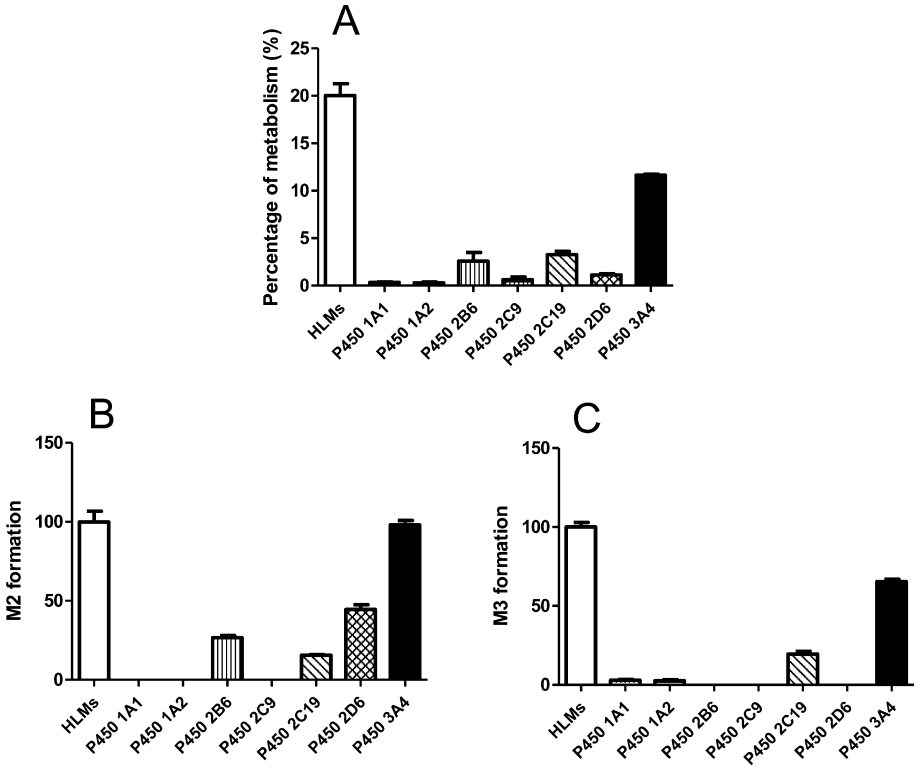

Figure 7. Percentage of metabolism (A), M2 (B), and M3 (C) formation rates of PLA in human liver microsomes and different human P450 enzymes. M2 and M3 formation rates in human liver microsomes were normalized to be 100, while the percentage of M2 and M3 formation rates in different human P450 enzymes were calculated by comparing with that in human liver microsomes.

Enzymes Mediating the Metabolism of PLA in Rats. As demonstrated in Figure 2B, all metabolites of PLA formed were via NADPH-dependent oxidative reaction, which might be catalyzed by microsomal enzyme P450s and/or FMOs. Further studies to quantify the changes in metabolic rate and the formation of M2 and M3 caused by different P450 or FMO inhibitors were conducted using rat liver microsomes. Formation of M1 was not quantified due to its trace amount generated. The metabolic rate of PLA with rat liver microsomes (about 48%, Figure 6A) was higher than that with rat hepatic S9 incubation (about 38%, Figure 3A), further indicating that the microsomal enzymes mediated metabolism. Moreover, the results (Figure 6A) obtained from the inhibitory study demonstrated that SKF 525A (a nonselective P450 inhibitor) significantly inhibited the metabolism of PLA and the formation of both M2 and M3, while methimazole (a nonspecific FMO inhibitor) did not show a significant inhibitory effect, indicating that P450 enzymes, but not FMO, mediated the hepatic metabolism of PLA and the formation of all metabolites identified.

Furthermore, the P450 enzymes involved in the metabolism of PLA were also investigated using various specific inhibitors. As shown in Figure 6B, except for P450 2E1 inhibitor, all other inhibitors significantly inhibited the metabolism of PLA. The formation of M2 was mainly catalyzed by P450 1A1/2, 2B, and 3A, while the formation of M3 was mainly mediated by P450 1A1/2, 2D, and 3A. Among all the P450 enzymes involved, P450 3A and P450 2D subfamilies played the most important role in the hepatic metabolism of PLA, and P450 3A was involved in the formations of both M2 and M3.

Metabolism of PLA in Human Liver Microsomes and Recombinant Supersomes. The metabolism of PLA was further investigated in human liver microsomes. The results demonstrated that the metabolic pathways of PLA were the same in both rat and human with M3 as predominant metabolite, although the metabolic rate of PLA was significantly lower than that in rat liver microsomes (human liver microsomes = 20%, Figure 7A, versus rat liver microsomes = 48%, Figure 6A1). Similarly, P450 3A, specifically P450 3A4 in a recombinant human supersome test, showed significantly high activity in mediating the formations of both M2 and M3 as well as the overall metabolism of PLA. In addition, the formation of the predominant M3 was also catalyzed by P450 2C19, 1A1, and 1A2, while the formation of M2 was also mediated by P450 2D6, 2B6, and 2C19.

■ DISCUSSION

PAs are probably the most common naturally occurring toxins affecting humans due to the wide distribution and high risk of unwitting consumption of PA-contaminated natural products. The two types of unsaturated PAs are hepatotoxic due to the hepatic metabolic activation, while the platynecine type of saturated PAs are known to not cause hepatotoxicity. However, although Mattock and White[25] proposed the absence of metabolic activation in nontoxic platynecine-type PAs about 30 years ago, the knowledge of their detailed metabolic pathways is largely unknown, mainly because the unstable pyrrolic esters produced by metabolic activation cannot be determined. Our present study on PLA, a representative platynecine-type PA, delineated the detailed metabolic pathways of platynecine-type PAs. Our findings revealed that, although there were no significant differences in hepatic metabolic rates between nontoxic and toxic PAs, not the saturated PAs but only the unsaturated PAs underwent

dx.doi.org/10.1021/tx4004159 | Chem. Res. Toxicol. 2014, 27, 7−16

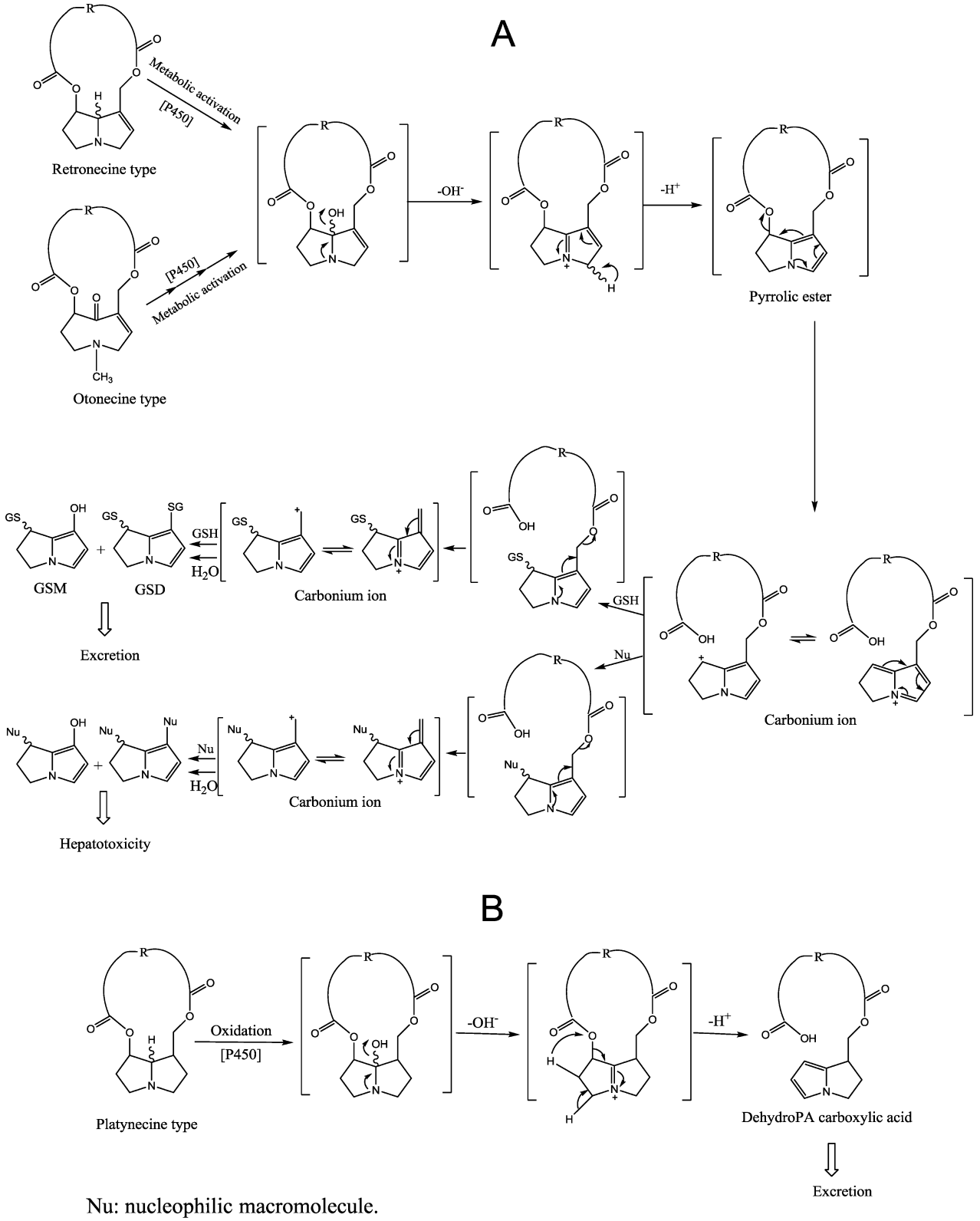

Figure 8. Different oxidative metabolic pathways of three types of PAs with illustrations of the metabolic activation of unsaturated toxic PAs (A) and the formation of excreted metabolite of saturated nontoxic PAs (B).

metabolic activation to generate the reactive pyrrole esters. This evidence was based on the unequivocal measurement of GSM, the pyrrole ester-derived glutathione conjugate (Figure 8), which directly correlates with the formation of the reactive pyrrole esters, the primary causative intermediates for hepatotoxicity via the intervention between pyrrole esters and cellular macromolecules. Therefore, with a direct comparison of the unsaturated toxic PAs, we provided the solid evidence to prove

dx.doi.org/10.1021/tx4004159 | *Chem. Res. Toxicol.* 2014, 27, 7−16

Mattocks' hypothesis[25] in that metabolic activation is absent in nontoxic platynecine-type PAs, which is confirmed as the primary reason for the nontoxic nature of platynecine-type PAs.

Furthermore, with a similar metabolic rate but without formation of the reactive pyrrole esters, the other metabolites that are different from those produced by toxic unsaturated PAs were generated by nontoxic saturated PAs. These metabolites were identified to be all oxidative metabolites. Moreover, the predominant metabolites M3 and M4 of PLA and NPLA were unequivocally identified as dehydroPLA carboxylic acid and dehydroNPLA carboxylic acid, respectively. The oxidation pathways of PLA are proposed as shown in Figure 5. Previously, a similar oxidative metabolite was also found to be the major nontoxic metabolite of another platynecine-type PA, rosmarinine, in both rat liver microsomal incubation and liver obtained from male rats treated with rosmarinine.[25] More importantly, in the same study, this metabolite was also determined in the urine of male rats treated with rosmarinine,[25] indicating that this novel and predominant metabolite was water-soluble and thus suspected to be readily excreted without causing toxicity. However, further in vivo studies of more PAs of this type to confirm their excretion are warranted.

It has been well-known that the metabolic formation of reactive pyrrolic esters of both retronecine type and otonecine type of toxic PAs is catalyzed mainly by P450 3A4 in human and P450 A1/2 (equivalent to P450 3A4 in human) in rats.[2,3] Our present results also demonstrated that all metabolites of PLA generated from the oxidative metabolism were mediated mainly by P450 3A as well as other P450 enzymes with much less activities in both human and rat microsomal metabolism, and the formation of the predominant M3 was mediated significantly by P450 3A4 (human) and P450 3A1/2 (rat). These findings confirmed that the hepatic enzymes mediating the major oxidative metabolism of all PAs regardless of their toxic properties were the same, although the metabolic activation to the reactive pyrrolic esters occurred only in the toxic unsaturated PAs, while the detoxification pathway to a nontoxic polar metabolite was predominant in the saturated PAs. As a result, the enzyme mediating the major hepatic metabolism is unlikely to be the cause for the differences in hepatotoxicity of different types of PAs.

Therefore, it is confirmed as previously suggested by others[2,3,14] that the structural differences in the necine bases of different PAs are the key determinant governing the toxicity. As illustrated in Figure 8A, in the case of retronecine-type PAs, metabolic activation involves the first hydroxylation at the C-8 position to form the 8-hydroxynecine derivatives followed by spontaneous dehydration facilitated by the conjugated system between unpaired electrons in nitrogen and the 1,2-double bond to produce the corresponding dehydropyrrolizidine intermediates (pyrrolic esters), which have two reactive alkylating groups (7-ester and 9-ester groups) to induce hepatotoxicity through intervention between cellular macromolecules and C-7 carbonium ion followed by C-9 carbonium ion to form different adducts.[2] Similarly, PLA can also be metabolized into a dehydropyrrolizidine derivative via two steps (Figure 8B). The first step is also the hydroxylation at the C-8 position; however, without the 1,2-double bond involved conjugated system to facilitate the second step of spontaneous dehydration in the necine base, it could only undergo the cleavage of the 7-ester group to generate a dehydroPA carboxylic acid. Importantly, the resultant dehydroPA carboxylic acid cannot exert hepatotoxicity because, first, it no longer has alkylating properties due to the disappearance of the ability to generate C-7 carbonium ion and, second, it can be readily excreted due to its aqueous solubility.

In conclusion, on the basis of the results of our comparable metabolic study using individual PAs representing three different types of PAs, we provided, for the first time, the solid evidence to prove the hypothesis, which had been proposed for a long time in that the primary determinant to distinguish nontoxic from toxic PAs is the structural differences in the necine base. The prerequisite of two types of toxic PAs is, regardless their different structures, the 1,2-double bond unsaturated necine base, which is metabolically activated via P450 enzymes, in particular, P450 3A4, mediated oxidation in the liver to generate reactive pyrrolic esters followed by their intervention with macromolecules, leading to hepatotoxicity. The key feature of nontoxic platynecine-type PAs is the saturated necine base, which does not undergo metabolic activation to generate reactive pyrrolic esters. On the other hand, the saturated platynecine-type PA also underwent the P450 3A4 mediated oxidative metabolism to form a predominant nonreactive and readily excreted soluble metabolite. Our findings delineated the metabolic pathway responsible for the nontoxic nature of platynecine-type PAs.

■ ASSOCIATED CONTENT

Supporting Information

Mass spectra of M4 and NMR spectra of M3. This material is available free of charge via the Internet at http://pubs.acs.org.

■ AUTHOR INFORMATION

Corresponding Author

*Tel.: +852 39436824. Fax: +852 26035139. E-mail: linge@cuhk.edu.hk.

Funding

The present studies were supported by Research Grant Council of Hong Kong (GRF Grant Nos. 471310 and 469712) and CUHK Direct Grant 2041744.

Notes

The authors declare no competing financial interest.

■ ABBREVIATIONS

PA, pyrrolizidine alkaloid; PLA, platyphylline; NPLA, neoplatyphylline; RET, retrorsine; CLI, clivorine; GSH, glutathione; GSM, 7-glutathionyldehydroretronecine; GSD, 7,9-diglutathionyldehydroretronecine; P450, cytochrome P450; FMO, flavin-containing mono-oxygenases

■ REFERENCES

(1) Chung, W. G., and Buhler, D. R. (1994) The effect of spironolactone treatment on the cytochrome P450-mediated metabolism of the pyrrolizidine alkaloid senecionine by hepatic microsomes from rats and guinea pigs. *Toxicol. Appl. Pharmacol. 127*, 314−319.

(2) Fu, P. P., Xia, Q., Lin, G., and Chou, M. W. (2004) Pyrrolizidine alkaloids—genotoxicity, metabolism enzymes, metabolic activation, and mechanisms. *Drug. Metab. Rev. 36*, 1−55.

(3) Li, N., Xia, Q., Ruan, J., Fu, P. P., and Lin, G. (2011) Hepatotoxicity and tumorigenicity induced by metabolic activation of pyrrolizidine alkaloids in herbs. *Curr. Drug Metab. 12*, 823−834.

(4) Lin, G., Wang, J. Y., Li, N., Li, M., Gao, H., Ji, Y., Zhang, F., Wang, H., Zhou, Y., Ye, Y., Xu, H. X., and Zheng, J. (2011) Hepatic sinusoidal obstruction syndrome associated with consumption of *Gynura segetum*. *J. Hepatol. 54*, 666−673.

(5) Gao, H., Li, N., Wang, J. Y., Zhang, S. C., and Lin, G. (2012) Definitive diagnosis of hepatic sinusoidal obstruction syndrome induced by pyrrolizidine alkaloids. *J. Dig. Dis. 13*, 33−39.
(6) Yang, Y. C., Yan, J., Doerge, D. R., Chan, P. C., Fu, P. P., and Chou, M. W. (2001) Metabolic activation of the tumorigenic pyrrolizidine alkaloid, riddelliine, leading to DNA adduct formation in vivo. *Chem. Res. Toxicol. 14*, 101−109.
(7) Chou, M. W., Jian, Y., Williams, L. D., Xia, Q., Churchwell, M., Doerge, D. R., and Fu, P. P. (2003) Identification of DNA adducts derived from riddelliine, a carcinogenic pyrrolizidine alkaloid. *Chem. Res. Toxicol. 16*, 1130−1137.
(8) Fu, P. P., Chou, M. W., Churchwell, M., Wang, Y., Zhao, Y., Xia, Q., Gamboa da Costa, G., Marques, M. M., Beland, F. A., and Doerge, D. R. (2010) High-performance liquid chromatography electrospray ionization tandem mass spectrometry for the detection and quantitation of pyrrolizidine alkaloid-derived DNA adducts in vitro and in vivo. *Chem. Res. Toxicol. 23*, 637−652.
(9) Xia, Q., Chou, M. W., Lin, G., and Fu, P. P. (2004) Metabolic formation of DHP-derived DNA adducts from a representative otonecine type pyrrolizidine alkaloid clivorine and the extract of *Ligularia hodgsonnii* hook. *Chem. Res. Toxicol. 17*, 702−708.
(10) Lin, G., Tang, J., Liu, X. Q., Jiang, Y., and Zheng, J. (2007) Deacetylclivorine: a gender-selective metabolite of clivorine formed in female Sprague-Dawley rat liver microsomes. *Drug Metab. Dispos. 35*, 607−613.
(11) Lin, G., Cui, Y. Y., and Hawes, E. M. (1998) Microsomal formation of a pyrrolic alcohol glutathione conjugate of clivorine. Firm evidence for the formation of a pyrrolic metabolite of an otonecine-type pyrrolizidine alkaloid. *Drug Metab. Dispos. 26*, 181−184.
(12) Lin, G., Cui, Y. Y., and Hawes, E. M. (2000) Characterization of rat liver microsomal metabolites of clivorine, an hepatotoxic otonecine-type pyrrolizidine alkaloid. *Drug Metab. Dispos. 28*, 1475−1483.
(13) Hartmann, T., Theuring, C., Beuerle, T., Klewer, N., Schulz, S., Singer, M. S., and Bernays, E. A. (2005) Specific recognition, detoxification and metabolism of pyrrolizidine alkaloids by the polyphagous arctiid *Estigmene acrea*. *Insect Biochem. Mol. Biol. 35*, 391−411.
(14) Mattocks, A. R. (1968) Toxicity of pyrrolizidine alkaloids. *Nature 217*, 723−728.
(15) Schoental, R. (1957) Hepatotoxic action of pyrrolizidine (Senecio) alkaloids in relation to their structure. *Nature 179*, 361−363.
(16) Chen, K. K., Harris, P. B., and Rose, C. L. (1939) The action and toxicity of platyphylline and seneciphylline. *J. Pharmacol. Exp. Ther. 68*, 130−140.
(17) Lin, G., Rose, P., Chatson, K. B., Hawes, E. M., Zhao, X. G., and Wang, Z. T. (2000) Characterization of two structural forms of otonecine-type pyrrolizidine alkaloids from *Ligularia hodgsonii* by NMR spectroscopy. *J. Nat. Prod. 63*, 857−860.
(18) Omura, T., and Sato, R. (1964) The carbon monoxide-binding pigment of liver microsomes. I. Evidence for its hemoprotein nature. *J. Biol. Chem. 239*, 2370−2378.
(19) Ma, B., Yin, C., Yang, D., and Lin, G. (2012) Effect of structural modification on the gastrointestinal stability and hepatic metabolism of α-aminoxy peptides. *Amino Acids 43*, 2073−2085.
(20) Chu, P. S., Lame, M. W., and Segall, H. J. (1993) In vivo metabolism of retrorsine and retrorsine-*N*-oxide. *Arch. Toxicol. 67*, 39−43.
(21) Li, S. L., Lin, G., Fu, P. P., Chan, C. L., Li, M., Jiang, Z. H., and Zhao, Z. Z. (2008) Identification of five hepatotoxic pyrrolizidine alkaloids in a commonly used traditional Chinese medicinal herb, Herba *Senecionis scandentis* (Qianliguang). *Rapid Commun. Mass Spectrom. 22*, 591−602.
(22) Ruan, J., Li, N., Xia, Q., Fu, P. P., Peng, S., Ye, Y., and Lin, G. (2012) Characteristic ion clusters as determinants for the identification of pyrrolizidine alkaloid *N*-oxides in pyrrolizidine alkaloid-containing natural products using HPLC-MS analysis. *J. Mass. Spectrom. 47*, 331−337.
(23) Asada, Y., Furuya, T., and Murakami, N. (1981) Pyrrolizidine alkaloids from *Ligularia japonica*. *Planta Med. 42*, 202−203.
(24) Roder, E., Wiedenfeld, H., and Jost, E. J. (1982) Pyrrolizidinalkaloide aus *Senecio congestus*. *Planta Med. 44*, 182−183.
(25) Mattocks, A. R., and White, I. N. (1971) Pyrrolic metabolites from non-toxic pyrrolizidine alkaloids. *Nat. New Biol. 231*, 114−115.